{ TC "' CHAPTER 2 : PHOTOVOLTAIC CELLS MODELS'" \L 1 }CHAPTER TWO

PHOTOVOLTAIC CELL MODELS

2.1 Introduction{ TC "2.1 Introduction" \l 2 }

In this chapter, both crystal silicon (C-Si) solar cell and amorphous silicon (a-Si) solar cell models, the most popular in the PV market, are discussed. Techniques to calculate the parameters of a-Si cell are presented. Also an improved simulation algorithm of a PV system that can be used in EES and TRNSYS programs was introduced.

2.2 Previous C-Si Cell Model{ TC "2.2 Previous C-Si Cell Model" \l 2 }

Since the rapid evolution of PV technology in the 1950s, crystal silicon has remained the 'workhorse' for outdoor applications, withstanding challenges by thin-film cells based on cadmium sulfide in the 1970s and on amorphous silicon alloy in the 1980s. Improved cell designs and increasingly streamlined manufacturing, combined with excellent field reliability and stability, ensure an ongoing role for this technology into the future. Figure 2.1 shows the performance levels reached over the 50 years period of development, with the rate of progress varying quite significantly with material understanding.

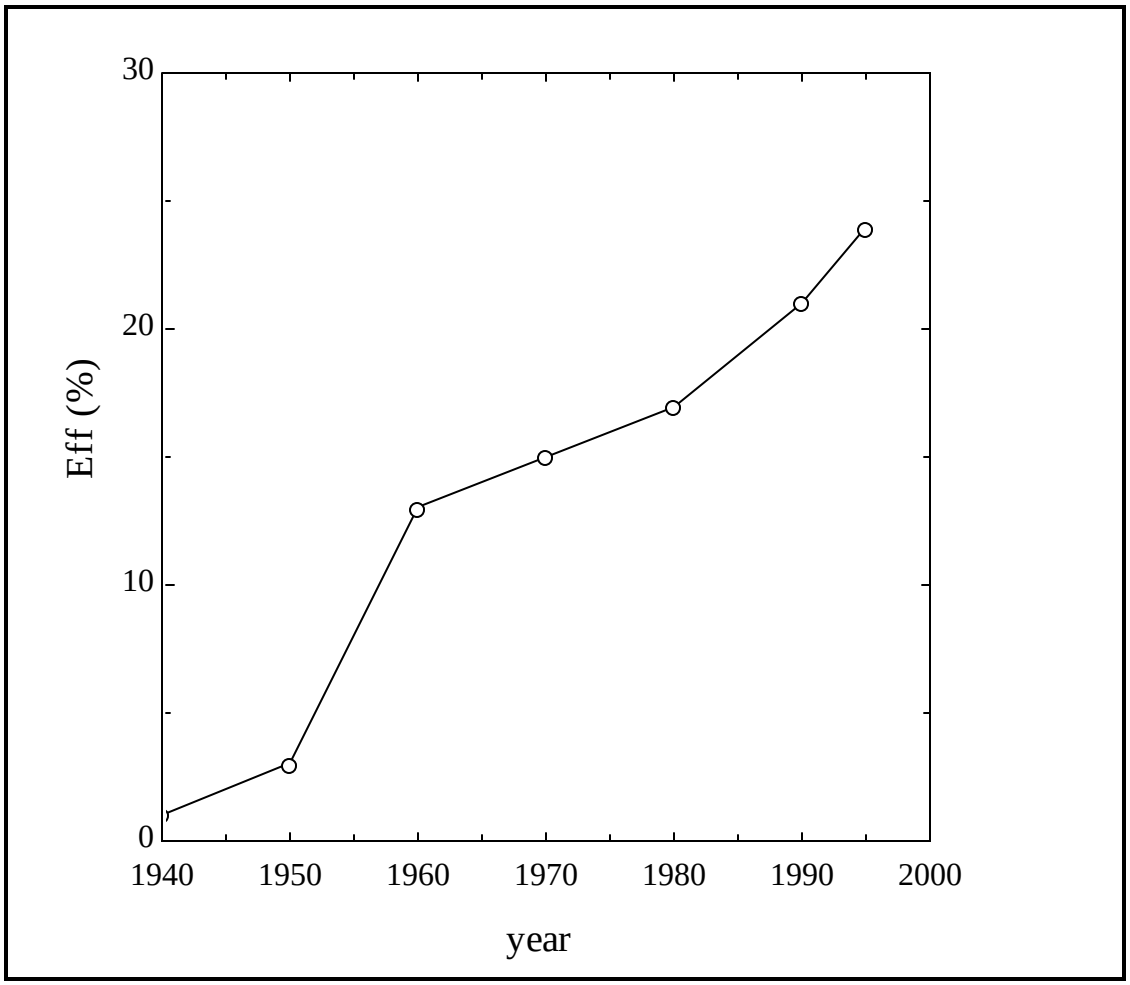

Figure 2.1 Evolution of Silicon solar cell efficiencies (Green, 1993)**{** TC "Figure 2.1 Evolution of Silicon solar cell efficiencies (Green, 1993)" \l 6 **}**

A photovoltaic system is composed of building blocks that are electronic devices (such as diodes), an assembly of electronic devices (such as PV modules), electronic circuits or systems (such as power-conditioning equipment) or energy storage elements (such as batteries). For all the individual components there exist analytical or quasi-analytical models to predict the electrical behavior under arbitrary conditions of radiation, operating temperature or power level. Therefore, the simulation of PV systems is formally the same problem as the simulation of any other electronic circuit or system.

The solar cell is a nonlinear power source. The output current and voltage depend on the radiation level and temperature as shown in Figure 2.2. Whenever the weather condition is changed, the operating point of solar cell will change.

.

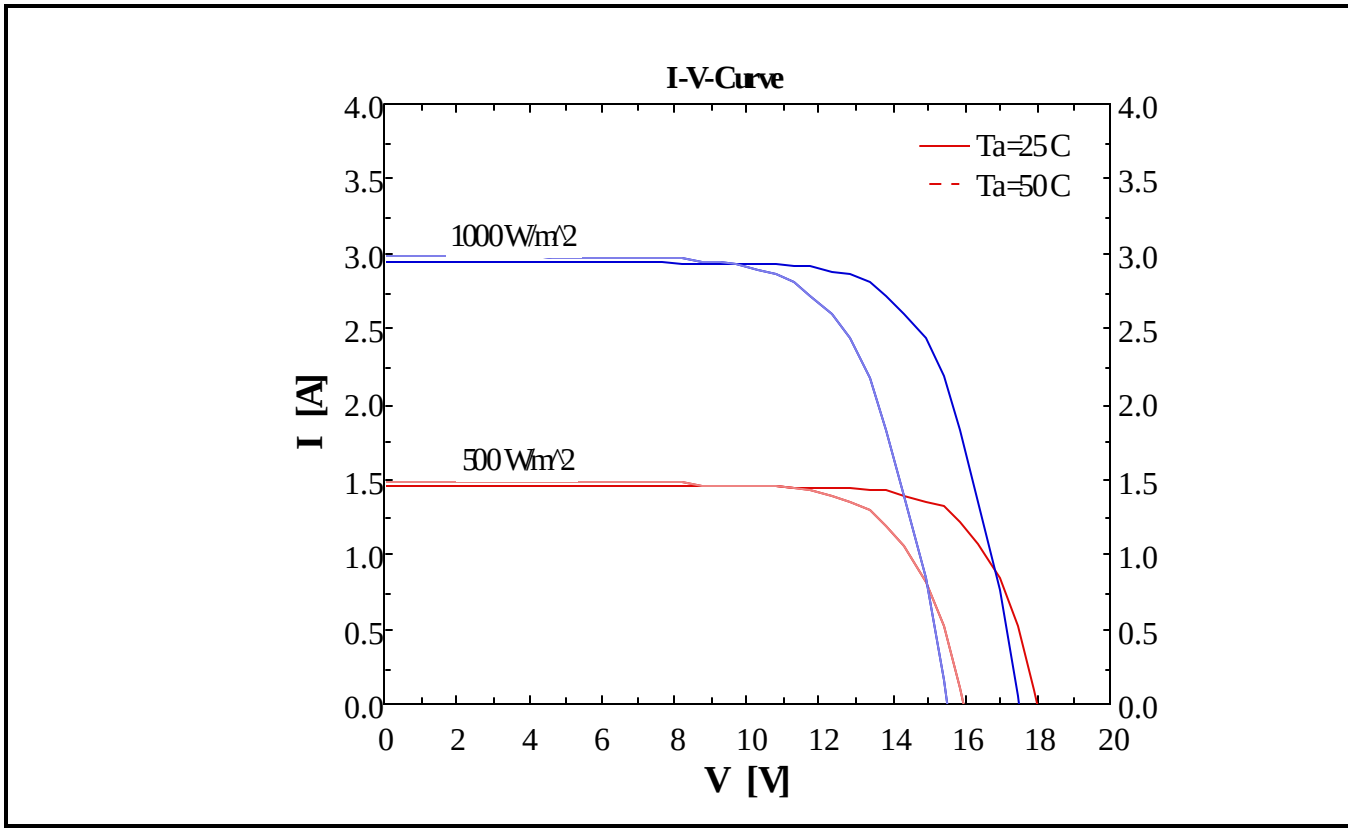

Figure 2.2 The I-V curve of a solar cell under different radiation and temperature.**{** TC "Figure 2.2 The I-V curve of a solar cell under different radiation and temperature." \l 6 **}**

(Al-Ibrahim,1996)

To predict the performance of a solar cell, it is important to create a solar cell model. Many researchers have investigated the photovoltaic cell by using different models for the simulation and design purpose (e.g. M. Wolf, 1977 and Appelbaum, 1979).

The solar cell structure can be represented by the equivalent circuit as shown in Figure 2.3.

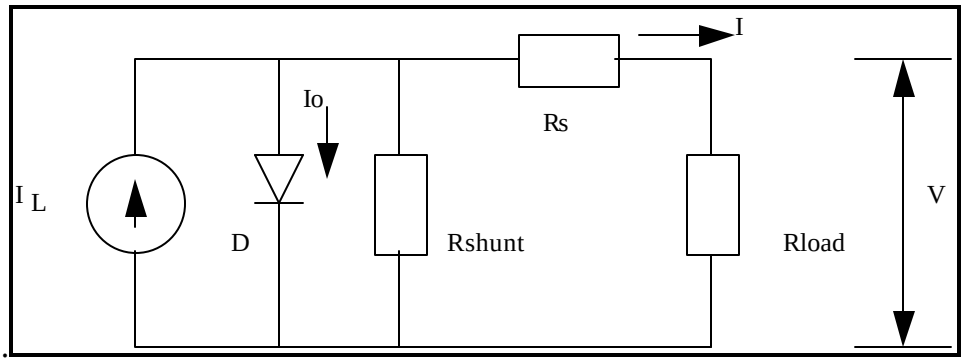

Figure 2.3 Equivalent circuit of a solar cell { TC "Figure 2.3 Equivalent circuit of a solar cell " \l 6 }

A general solar cell model which is based on the circuit in Figure 2.3 can be written as

$$I = I_L - I_o\left\{exp\left(\frac{V+IR_s}{A}\right)-1\right\}-\frac{V+IR_s}{R_{sh}} \qquad (2.1)$$

where

I_L	Light current	(A){ TC "I_L Light current (A)" \l 7 }
I_o	Dark current	(A){ TC "I_o Dark current (A)" \l 7 }
I	Operation current	(A){ TC "I Operation current (A)" \l 7 }
V	Operation voltage	(V){ TC "V Operation voltage (V)" \l 7 }
Rs	Series resistance	( ){ TC "Rs Series resistance ( )" \l 7 }
R_{shunt}	Shunt resistance	( ){ TC "R_{shunt} Shunt resistance ( )" \l 7 }

A Thermal voltage (V){ TC "A Thermal voltage (V)" \l 7 }

In Equation 2.1 I_L, I_o, R_s, R_{sh}, and A are 5 parameters that depend on the radiation and temperature. Therefore the simulation of a PV cell must focus on how to find those five parameters at different weather conditions.

Unfortunately we are only given three data points from the manufactures, i.e. the open circuit voltage, the short circuit current and the maximum power point. This information is not enough to find those 5 parameters.

Townsend (1989), Eckstein (1990), Al-Ibrahim (1996), analyzed and figured out a 4 parameter model which can be used in a TRNSYS program.

This model neglected the shunt resistance R_{sh} because the R_{sh} is very large compared with the R_s for the C-Si cell. Therefore the Equation 2.1 can be rewritten as

$$I = I_L - Io\left\{exp\left(\frac{V + IR_s}{A}\right) - 1\right\} \qquad (2.2)$$

where

I_L Light current (A){ TC "I_L Light current (A)" \l 7 }

I_o Dark current (A){ TC "I_o Dark current (A)" \l 7 }

I Operation current (A){ TC "I Operation current (A)" \l 7 }

V Operation voltage (V){ TC "V Operation voltage (V)" \l 7 }

R_S Series resistance ( ){ TC "R_S Series resistance ( )" \l 7 }

Now only the 4 parameters, I_L, I_O, R_S, and A, need to be evaluated. A method to calculate these parameters has been developed by Townsend (1989) and Eckstein (1990). Since there are 4 unknown parameters, 4 conditions of I and V are needed. Manufacturers usually provide I and V at short circuit, at open circuit and at maximum power point. The 4th condition comes from the knowledge of μ_{VOC} and $\mu_{ISC.}$ Equation 2.3 - 2.6 are used to calculate those parameters of PV cells at standard condition based on the experimental data provided by the manufacturer.

$$I_{Lref} = I_{scref} \tag{2.3}$$

$$I_{oref} = \frac{I_{Lref}}{exp\left(\frac{V_{ocref}}{A_{ref}}\right) - 1} \tag{2.4}$$

$$R_{sref} = \frac{A_{ref} ln\left(1 - \frac{I_{mpref}}{I_{Lref}}\right) - V_{mpref} + V_{ocref}}{I_{mpref}} \tag{2.5}$$

$$A = \frac{\mu_{Voc} T_{cref} - V_{ocref} + E_g N_s}{\frac{T_{cref} \mu_{Isc}}{I_{Lref}} - 3} \tag{2.6}$$

where

{ TC "" \l 7 } I_{Lref} Light current at reference condition

(A)

{ TC "" \l 7 } I_{scref} Short circuit current at reference condition (A)

{ TC "" \l 7 } I_{oref} Reverse saturation current at reference condition (A)

{ TC "" \l 7 } V_{ocref} Open circuit voltage at reference condition (V)

{ TC "" \l 7 } A_{ref} Thermal voltage at reference condition (V)

{ TC "" \l 7 } R_{sref} Series resistance at reference condition ( )

{ TC "" \l 7 } I_{mpref} Maximum power current at reference condition current(A)

{ TC "" \l 7 } V_{mpref} Maximum voltage at reference condition (V)

{ TC "" \l 7 } μ_{Voc} Temperature coefficient of cell voltage (V/C)

{ TC "" \l 7 } μ_{Isc} Temperature coefficient of cell current (A/C)

.c7 T_{cref} Cell temperature at reference condition (C)

{ TC "" \l 7 } E_q Band gap of silicon (eV)

{ TC "" \l 7 } N_s Number of cells in series in one module

Whenever weather conditions change, the cell parameters change and can be estimated from the following equations.

$$I_L = \left(\frac{G}{G_{ref}} \right) \left\{ I_{L,ref} + \mu_{Isc} \left(T_c - T_{c,ref} \right) \right\} \qquad (2.7)$$

$$I_o = I_{o,ref} \left(\frac{T_c}{T_{c,ref}} \right)^3 exp\left(\left(\frac{N_{sc} E_q}{A} \right) \left(1 - \frac{T_{c,ref}}{T_c} \right) \right) \qquad (2.8)$$

$$R_s = R_{sref} \tag{2.9}$$

$$A = A_{ref} \frac{T_c}{T_{cref}} \tag{2.10}$$

where

{ TC "" \l 7 } G	Radiation level	(w/m^2)
{ TC "" \l 7 } G_{ref}	Reference radiation level (w/m^2)	
{ TC "" \l 7 } I_L	Light current at new condition	(A)
{ TC "" \l 7 } T_c	Cell temperature at new condition	(K)
{ TC "" \l 7 } I_o	Reverse saturation current at new condition	(A)
{ TC "" \l 7 } A	Thermal voltage at new condition	(V)

Using those parameters, the maximum power point of a PV array also can be evaluated by using the Newton-Raphson method.

2.3 TRNSYS PV Models{ TC "2.3 TRNSYS PV Models" \l 2 }

The steady state PV system operating point at the different radiation levels is at the intersection of the load line and the I-V characteristic of PV array as shown in Figure 2.4. In Figure 2.4, the load is a motor and the operating points of the PV system are at (V1, I1) and (V2, I2).

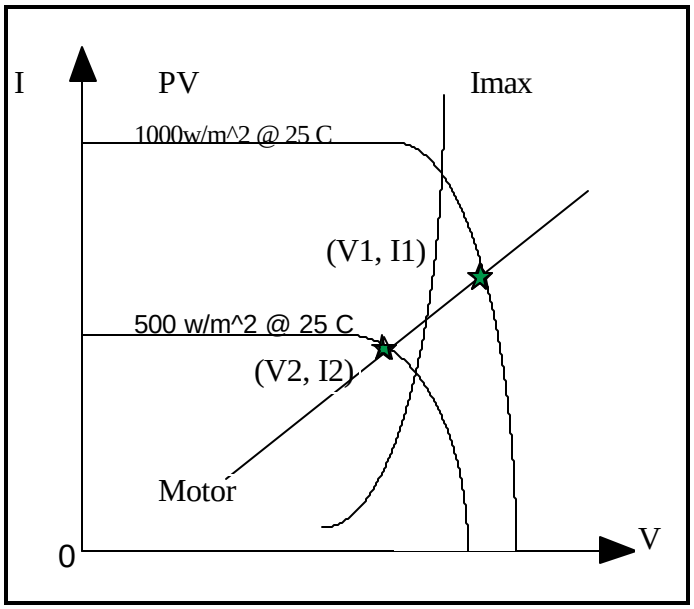

Figure 2.4 The operating points of PV system{ TC "Figure 2.4 The operating points of PV system" \l 6 }

To evaluate the performance of systems which includes a PV array, TRNSYS type 62 was developed and modified by Townsend (1989), Eckstein (1990), Al-Ibrahim (1996). The algorithm is represented in Figure 2.5. The operating point of the PV system can be calculated by iterating among PV model (equation 2.2) and other load models in the TRNSYS.

TRNSYS has been proven to be an accurate program in predicting and analyzing solar thermal and other energy system. It has a modular structure and consists of a variety of individual subroutines which present real physical devices. These components can be connected to systems and simulations can be run over different time periods. The TRNSYS simulation environment makes use of several terms for describing components, etc. These are:

Type: The component model, such as a pump. Each Type has a unique Type number in a simulation.

Unit: The nth copy of a type used in a simulation. Each Unit has a unique Unit number to distinguish it from the other Units of the same Type.

Deck: The input file used by TRNSYS to identify the Types used, the number of Units of each Type, and the interconnections between them. The deck can be either a simple deck describing the interconnections or it can be a TRNSED deck, which additionally describes a user-interface for the operation of the program.

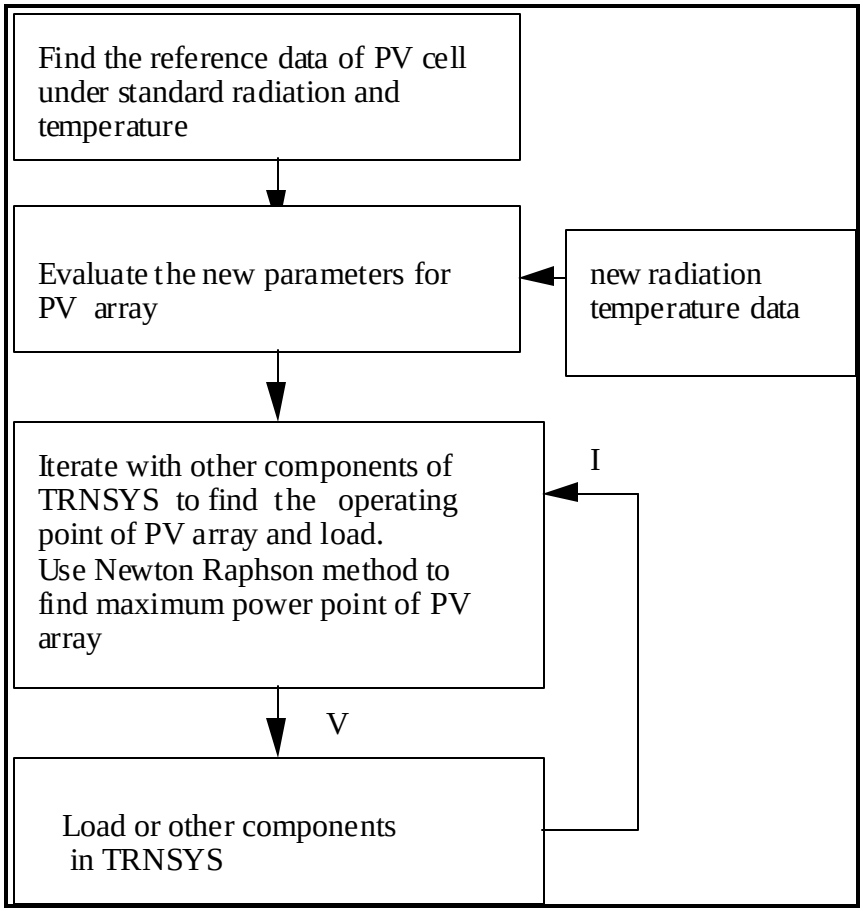

Figure 2.5 Previous PV system algorithm in TRNSYS{ TC "Figure 2.5 Previous PV system algorithm in TRNSYS" \l 6 }

Type 62 has two problems. One is the numerical method used among the PV model and load models. Because the PV model is a non linear fuction, the numerical method leads to calculation complexity. The second one is the solving process and it can not be controlled by user. Therefore the process can not be "monitored" by users. Sometime the iteration scheme is not stable.

2.3.1 TRNSYS Type 64{ TC "2.3.1 TRNSYS Type 64" \l 3 }

To reduce the calculation complexity and to improve the stability of simulation, a new algorithm has been developed and is shown in the Figure 2.6. Instead of using a numerical method to find the operating point, a linear search method is employed. In the improved model, the upper and lower boundary of the current value is determined at the new radiation level and temperature. The linear search method is used to find the operating point in the range of short circuit current and zero current because the operating point must be on the I-V curve of PV array, otherwise the system does not work. The program to find optimal configuration of PV modules has been developed and will be discussed in the chapter 5. The program can evaluate the best configuration of PV modules and guarantee the PV pumping system always works.

The linear search method, such as Bisection, Golden and fixed step methods, can be used to find the solution. At this stage, the fixed step method is employed. By reducing the current value from short circuit current to zero by fixed step, the voltage of the PV array and load is compared at each iteration. If the difference of voltage of PV array and the voltage of load is less than the tolerance, then the iteration will stop. Therefore the new algorithm can guarantee that operating point can be found.

The maximum power point (MPP) of the PV array is also evaluated. First, fix the radiation level and temperature information, the new short circuit current can be calculated. Second, the new short ciruit current and zero is set as the search boundary. The maximum power point can be found by the Golden linear search method. The flow chart of the algorithm for evaluating the maximum power point is shown in Figure 2.7.

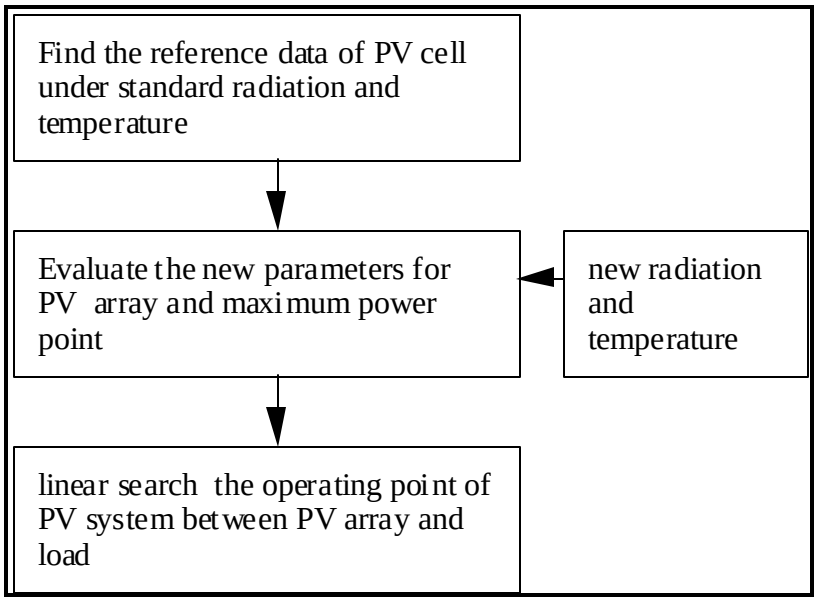

Figure 2.6 New PV System Algorithm in EES and TRNSYS{ TC " Figure 2.6 New PV System Algorithm in EES and TRNSYS" \l 6 }

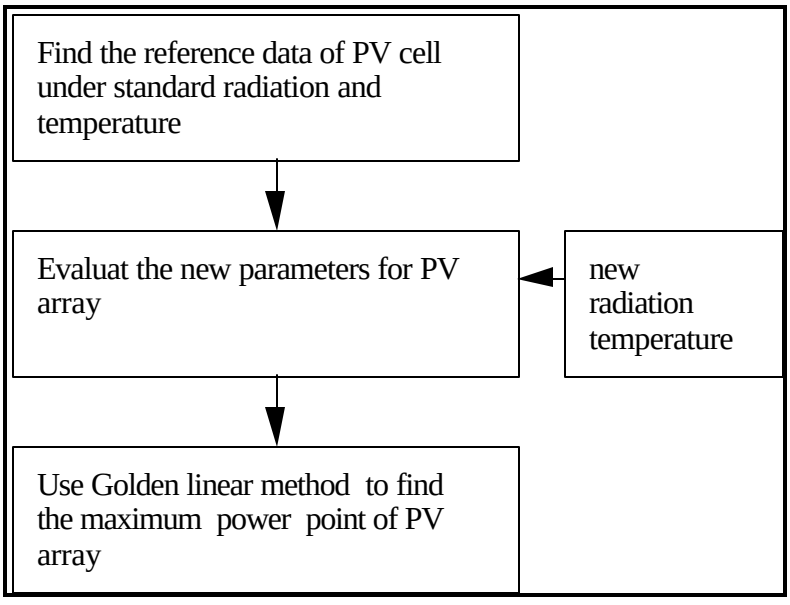

Figure 2.7 The flow chart of the new algorithm for evaluating the maximum power point of PV array{ TC "Figure 2.7 The flow chart of the new algorithm for evaluating the maximum power point of PV array" \l 6 }

Type 64 : PV System

The new algorithm is used in the TRNSYS type 64 and the EES. This type is different from old types that have been used in TRNSYS. It can accept other components of a PV system. This means that any load which has a known I-V characteristic can be integrated into this type. The operating point of the PV system can be found using the linear search method inside of this type instead of using iteration circle among PV array and load components. The flow chart of the type 64 is shown in Figure 2.8.

Parameters of type 64

1. Mode	Cell type	
2. G_{ref}	Reference radiation level	(W/m^2)
3. I_{Lref}	Light current at reference condition	(A)
4. I_{scref}	Short circuit current at reference condition	(A)
5. I_{oref}	Reverse saturation current at reference condition	(A)
6. V_{ocref}	Open circuit voltage at reference condition	(A)
7. A_{ref}	Thermal voltage at reference condition	(V)
8. R_{sref}	Series resistance at reference condition ( )	
9. I_{mpref}	Maximum power current at reference condition	current (A)
10. V_{mpref}	Maximum voltage at reference condition	(V)
11. MuV_{oc}	Temperature coefficient of cell voltage	(V/C)
12. MuI_{sc}	Temperature coefficient of cell current	(A/C)

13. T_{cref} Cell temperature at reference condition (C)

14. E_q Band gap of silicon (eV)

15. N_s Number of cells in series in one module

16. *N_S* Number of module in series

17. *N_P* Number of module in parallel

18. to 30 Parameters of pump or other loads

Input of type 64

1. Radiation level (W/m^2)

2 Temperature (C)

Output of type 64

1. Operating voltage of PV system (V)

2. Operating current of PV system (A)

3. Maximum current of PV system (A)

4. Maximum voltage of PV array (V)

5. Efficiency of PV array

6. Efficiency of PV system

7. Water output (Liter)

8. Water shortage (Liter)

9 and 10 are free

The type 64 only uses the radiation and temperature as the inputs. This new algorithm is also used in EES. EES and TRNSYS program codes are appended in Appendix A and B.

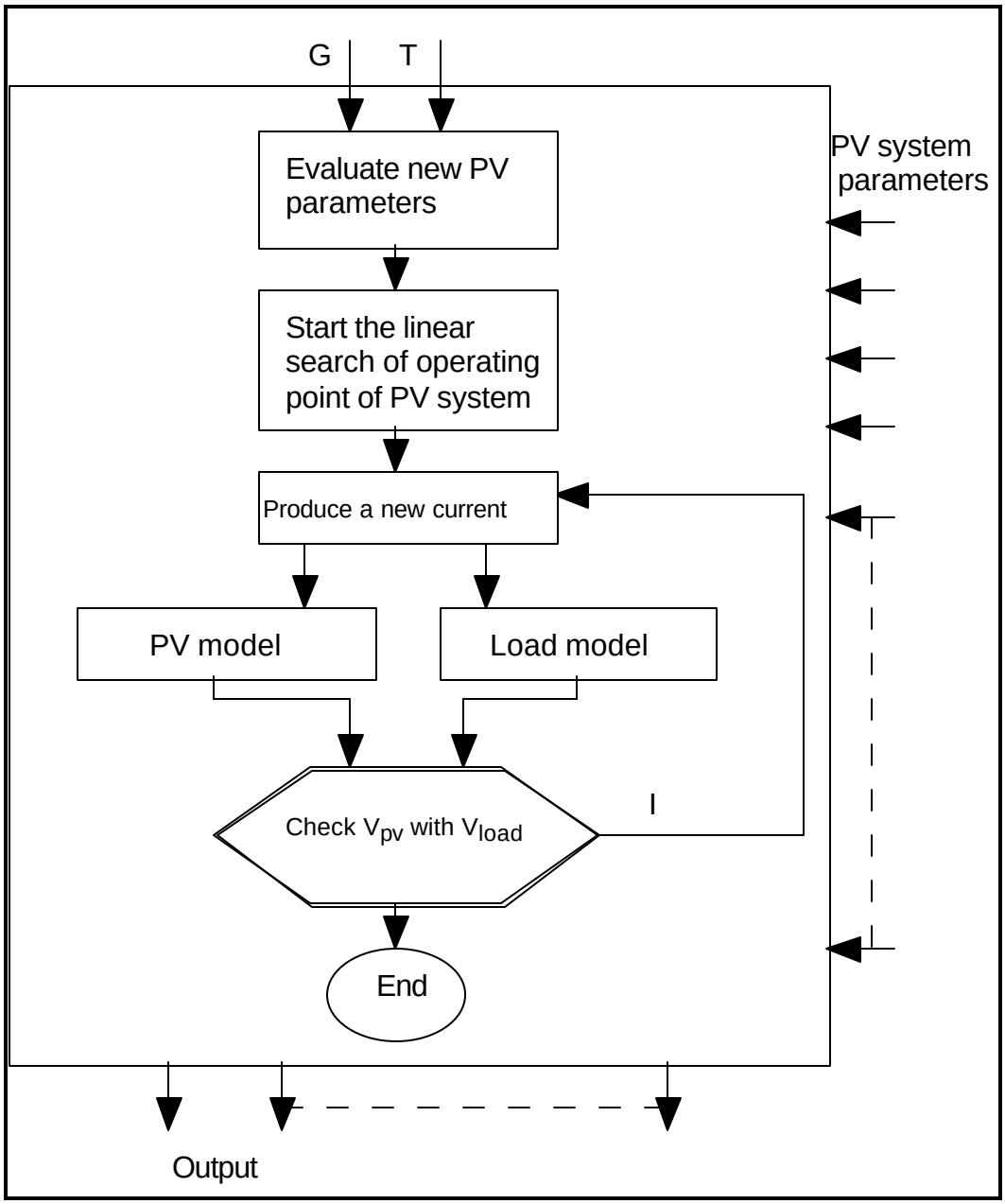

Figure 2.8 The structure of type 64**{** TC "Figure 2.8 The structure of type 64" \l 6 **}**

2.4 a-Si Cell Model{ TC "2.4 a-Si Cell Model" \l 2 }

The future of a-Si cell looks strong. Now it appears that commercial, multijunction a-Si modules could be in the 7% - 9% efficiency range in the near term and significant public announcements have been made by several companies (e.g. Solarex-Enron and United Solar) of 10-MW facilities to be built in the future. The a-Si could have a major impact on the PV market if its cost is in the \$1-\$2.5 W_p^{-1} range.

The use of a-Si solar cells has grown rapidly to a point where they now account for about 14% of all photovoltaic sales (on power basis). To date , a-Si photovoltaic modules dominate the market for indoor consumer products, but are mainly used outdoors in only low wattage, the most popular application is to use a a-Si module charging a battery. They are not generally being used in many of the higher wattage applications such as cathodic protection and water pumping etc. This is largely due to the fact that the stabilized conversion efficiency is not good. Usually efficiency of a-Si photovoltaic modules in range is 5% to 6% at beginning and decreases with exposure time. As a result, the total system cost is relatively high for applications where the cost of mounting, framing, wiring and land is high.

On the basis of measurement results from NREL, we have investigated the effects of modules performance parameters and environmental factors on the energy delivery of a-Si module and developed a model that can be used for calculating the performance estimation of a-Si model.

2.4.1 Unique performance of a-Si{ TC "2.4.1 Unique performance of a-Si" \l 3 }

1) Absorption mechanism of C-Si and a-Si

The most common semiconductor material for solar cell is silicon. Furthermore, crystalline silicon cells and amorphous silicon are outstanding representatives of bulk and barrier types.

C-Si and a-Si solar cells represent complementary cell types. The generation of photocarriers takes place in the semiconductor bulk (C-Si) or is confined to the barrier layer (a-Si). Carrier collection hence relies on the diffusion (C-Si) or drift (a-Si). The absorption length within a C-Si cell considerable exceeds the barrier-layer thickness. Photo generation thus occurs in field-free regions. The photocarriers diffuse to the junction. The filed spike attached to it sweeps the minority carriers through but blocks the majority carriers.

Carrier collection in a a-Si cell, in contrast, is confined to the barrier layer itself, i.e. the electron-hole separating layer, and therefore provides a field-driven photo current. Ideal C-Si and a-Si cells rely exclusively on photocarrier collection by diffusion and drift respectively. Real cells mostly combine the two collection mechanisms, though one of them may predominate.

A photocarrier can recombine before its arrival at the junction edge (C-Si cell) or during its passage through the barrier layer(barrier cell). In order to minimize recombination losses, the photocarrier diffusion lengths in a C-Si cell should exceed the thickness of the absorber regions extending over the edge absorption depth. The barrier width (derby length) and the photocarrier drift length should then exceed the absorption depth. Thin-film cell will profit from significant barrier collection. Since a very short distance is enough to collect the photo-generated carriers.

2) Loss mechanism of C-Si and a-Si

In a semiconductor, a photon which energy equals or is larger than the Eg of a solar cell only generates a carrier. Part of the energy of the photon is dissipated as heat. From the thermodynamic point of view, the loss mechanism of a crystalline cell can be considered as the pure radiation which is an explicit function depending on the operating voltage. In amorphous silicon a local electric field may arise from a static spatial variation due to lack of long range order , variations in density, or charged defects. Therefore the a-Si solar cell has a high density of state and form a recombination center at the end of conduction band and a valence band so called band tail state. In C-Si solar cell all atoms are in order therefore in the bandgap there is almost no density of state. This an important difference between C-Si and a-Si. See Figure 2.9.

The loss mechanism of a-Si solar cell can be summarized as following,

1). Band-tail recombination that a-Si has a large density of states in the band gap.

2). Deep-state denties

3). Defects of the material

An unique problem of a-Si cell is that its efficiency decreases along with the exposure time. The physical interpretation of the decay is the light induced degradation (Staebler-Wronsky Effect). The dominant parameter in the a-Si material degradation of modules is the decrease of the FF and Isc due to a reduced carrier collection length. This can be interpreted by two things, an increase in the number of dangling bonds in the midgap of the intrinsic a-Si layer limiting the ambipolar carrier lifetime, also because the Fermi level moves to thevalance band tail as shown in Figure 2.9.

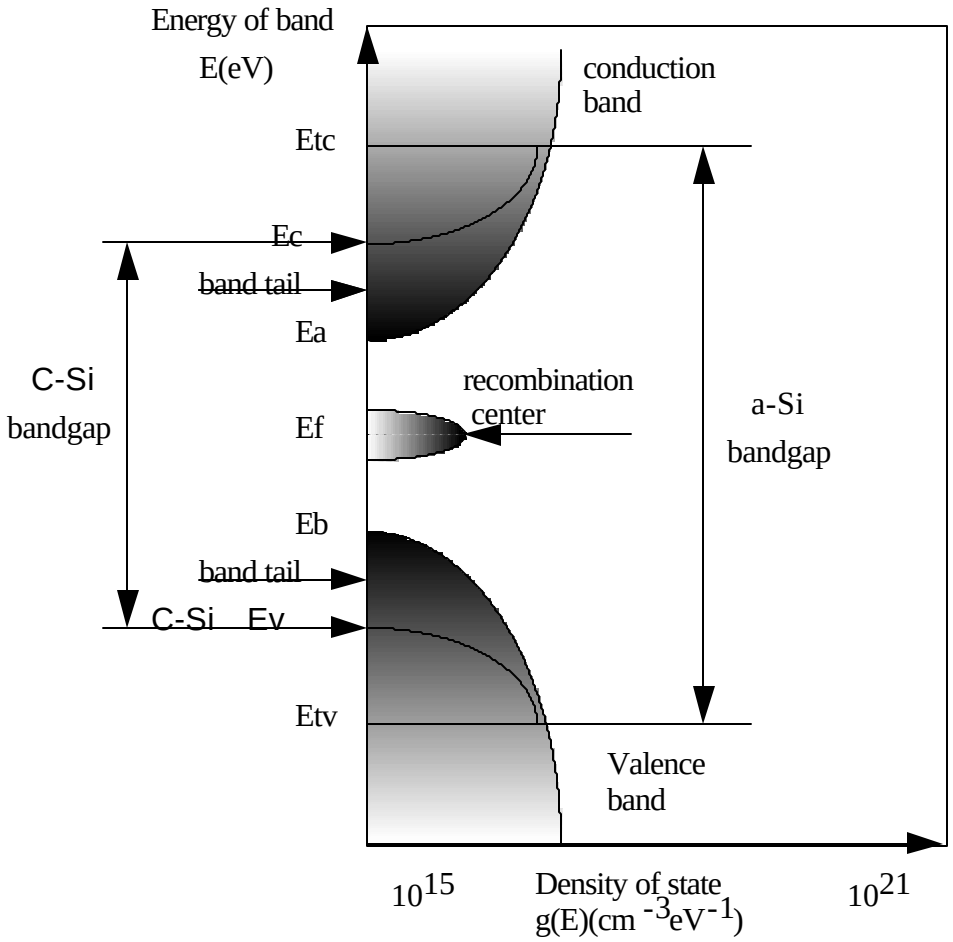

Figure 2.9 The bandgap of C-Si and a-Si cell{ TC "Figure 2.9 The bandgap of C-Si and a-Si cell" \l 6 }

The single junction creates metal stable defects via trapping or recombination events. Single - junction a-Si solar cells degrade by about 20% to 40% after a few months of exposure to sunlight. With multi -junction structures, the light induced degradation can be reduced to less than 10%, and stabilized conversion efficiencies of about 10% have been demonstrated in the lab. Low cost automated manufacturing lines indicates that thin film PV will soon start to penetrate high voltage markets such as water pumping.

2.4.2 Consideration of a-Si Cell Simulation{ TC "2.4.2 Consideration of a-Si Cell Simulation" \l 3 }

From an application point of view, the degradation of photovoltaic cell conversion efficiency mainly depends on the weather condition such as light intensity, spectral distribution and cell temperature. Performance of a-Si cell also depends on the exposure time.

The $E_{g\ of}$ a-Si cell is 1.7 eV. Because of the large bandgap, the high spectral response range of a-Si cell is in the range of 400 nm to 800 nm which spectral distribution does not change so much during different seasons (Green, 1993). It is also different from C-Si cell on this point. Therefore the spectral distribution will not be considered in our analysis.

On the other hand, the solar cell fabrication technology is being steadily improved, the deterioration problem can not be simply estimated based on the experiments with old ones. In this project only the radiation and temperature effects will be considered.

2.4.3 Model of a-Si Solar Cell{ TC "2.4.3 Model of a-Si Solar Cell" \l 3 }

In the present work, the objective is to investigate the effects of light intensity and temperature on the a-Si solar cell and to develop a model for simulating the characteristic of a-Si solar cell. Because mechanism of loss is different between a-Si and C-Si, the general model which is used to simulate C-Si solar cell should be modified.

The accurate performance of a PV solar cell can be represented by Equation.2.1 . Generally, Equation 2.1 can be applied to monocrystalline, polycrystalline and amorphous silicon solar cell.

The Solar Lab's model (Townsend, 1989) is good to simulate the C-Si cell. However the model does not fit measurement of a-Si solar cell very well. The main deviation is around the maximum power point because a-Si solar cell does not have as good of a fill factor as the crystal silicon cell does. In order to explain the low fill factors measured, the reduced series resistance of the solar cell and the shunt resistance which are lower than that of crystal silicon cell should be taken into account.

Therefore Equation 2.1 can be rewritten as following,

4 parameters equation

$$I = I_L - I_0 \left\{ exp\left(\frac{V}{A}\right) - 1 \right\} - \frac{V}{R_{sh}} \qquad (2.11)$$

where

Io	Reverse saturation current	(A)
I	Operating point of cell	(A)
I_L	Light current	(A)
V	Operating voltage of cell	(A)
A	Thermal voltage	(V)
R_{sh}	Series resistor of cell	( )

I_L, I_o, A and R_{sh} have to be solved. Rs is assumed as zero.

To solve the Equation 2.11, the derivation of 4 independent relations from Equation 2.9 can be made as following.

At open circuit point, $V=V_{OC}$, $I=0$

$$I_L = I_0\left\{exp\left(\frac{V_{oc}}{A}\right)-1\right\}+\frac{V_{oc}}{R_{sh}} \quad (2.12)$$

At short circuit point, $V=0$, $I = I_{SC}$

$$I_L = I_{sc} \quad (2.13)$$

At maximum power point, $V=V_m$, $I=I_m$

by rearranging Equation 2.9 we have

$$Im = I_L - I_o\left\{exp\left(\frac{Vm}{A}\right)-1\right\}+\frac{Vm}{R_{sh}} \quad (2.14)$$

On the I-V curve, when the $P=P_m$ which P is at maximum power point,

$$\frac{\partial P_m}{\partial I_m}=\frac{\partial V_m}{\partial I_m}I_m+V_m=0 \quad (2.15)$$

then

$$\frac{\partial V_m}{\partial I_m}=-\frac{V_m}{I_m} \quad (2.16)$$

The Equation 2.2 can be rewritten as,

$$Y(I,V) = I - I_L + X(V) = 0 \quad (2.17)$$

where

$$X(V) = I_0\left(exp\left(\frac{V}{A}\right) - 1\right) + \frac{V}{R_{sh}} \quad (2.18)$$

differential two sides,

$$\frac{\partial Y(I,V)}{\partial V}\frac{\partial V}{\partial I} + \frac{\partial Y(I,V)}{\partial I} = 0 \quad (2.19)$$

$$\frac{\partial Y(I,V)}{\partial V} = \frac{I_0}{A}exp\left(\frac{V}{A}\right) + \frac{1}{R_{sh}} \quad (2.20)$$

$$\frac{\partial Y(I,V)}{\partial I} = 1 \quad (2.21)$$

substitute the Equation 2.20, Equation 2.21 and Equation 2.16 into Equation 2.19, we have

$$1 - \frac{V_m}{I_m}\left(\frac{I_0}{A}exp\left(\frac{V_m}{A}\right) + \frac{1}{R_{sh}}\right) = 0 \quad (2.22)$$

Equation 2.22 will be the fourth equation for solving the 4 parameters model. An EES program was written for solving the four parameters based on the four equations. When the simulation of a PV system includes the a-Si module, the operating point of a PV system can be found by the procedure as shown in the Figure 2.11.

The procedure of the calculation is

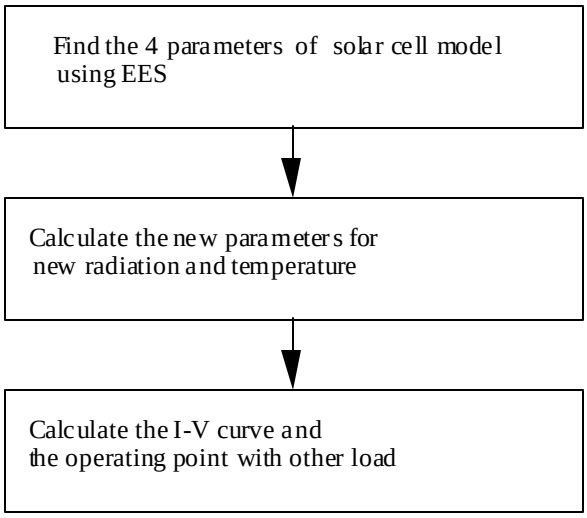

Figure 2.11 Flow chart of PV system including a-Si module{ TC "Figure 2.11 Flow chart of PV system including a-Si module" \l 6 }

The comparison between the measurement from NREL and the simulation at different radiation is shown in Figure 2.12. A good fit between the measurement and simulation is observed. Here the RMS difference which is defined as Equation 2.16 is .89%.

$$RMS\% = \left[\frac{\Sigma \left(I_{calculate} - I_{measure} \right)^2}{Total\ points} \right]^{1/2} \qquad (2.16)$$

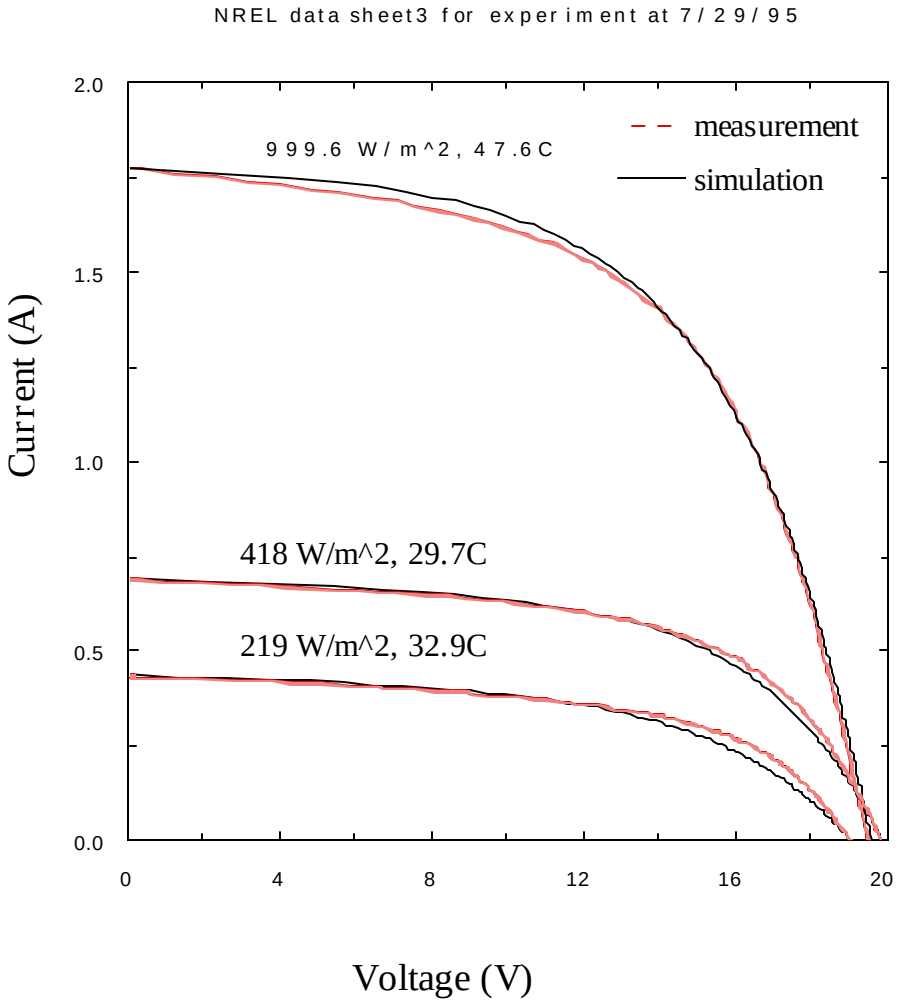

Figure 2.12 I-V curve comparison between measurement and simulation{ TC "Figure 2.12 I-V curve comparison between measurement and simulation" \l 6 }

Comparing the simulation results with measurements, there is a small difference. It proves the 4 parameter model by using Rsh instead of Rs can be used to simulate the a-Si cell. All parameters of this model have clear physical meaning.